Available online at www.sciencedirect.com
SCIENCE DIRECT®
Journal of Crystal Growth 254 (2003) 353–359
JOURNAL OF CRYSTAL GROWTH
www.elsevier.com/locate/jcrysgro

Observation of CuPt and CuAu I-type ordered structure in HgCdTe grown by isothermal vapour phase epitaxy

Myriam H. Aguirre[a,*], Horacio R. Cánepa[b], Noemí E. Walsöe de Reca[b]

[a] *Dpto de Química Inorgánica I, Facultad de Ciencias Químicas, Universidad Complutense, Av. Complutense s/n., 28040 Madrid, Spain*
[b] *CINSO-CONICET-CITEFA, Juan Bautista de La Salle 4397, B1603ALO Villa Martelli, Pcia de Buenos Aires, Argentina*

Accepted 8 April 2003
Communicated by J.B. Mullin

Abstract

Ordered structures, CuPt and CuAu I types in HgCdTe are reported for the first time. $Hg_{1-x}Cd_xTe$ thin crystals were grown by isothermal vapour phase epitaxy (ISOVPE) method on a CdTe substrate and they were observed by transmission electron microscopy (TEM) in planar view and cross-sectional geometries. Two variants of CuPt-type ordered structure were found in different microdomain sets on HgCdTe. Another superstructure observed was the CuAu I-type coexisting with CuPt domain structure.

PACS: 68.37.Lp; 68.55.Jk; 81.05.Dz; 81.15.Kk

Keywords: A1. Crystal structure; A3. Vapor phase epitaxy; B2. Semiconducting II–VI materials

1. Introduction

In general, chemically similar atoms are distributed randomly on their lattice sites in ternary crystals (e.g. In and Ga in GaInP or InGaAs, in III–V alloys or Hg and Cd in HgCdTe, II–VI alloys). Usually, III–V and II–VI alloys exhibit zinc blend structure, which is formed by two FCC lattices, displaced (1/4,1/4,1/4). One FCC lattice is occupied by elements from group III (II) and the other FCC lattice by the elements belonging to the group V (VI). On the other hand, using suitable growth conditions, self-ordered crystal can be spontaneously obtained [1]. Up to date, the ordered structures found in III–V alloys have been CuPt, CuAu forms and chalcopyrite types.

Predictions [2–6] and observations [7–12] of spontaneously ordered structures in III–V semiconducting compounds have generated considerable interest during the last 15 years for the following reasons: (1) the observed structures are unusual for semiconducting compounds, and (2) the energy gaps depend on the structure even for a fixed composition. Thus, by introducing ordering, a reduction of the energy gaps is obtained, so that the optoelectronic properties of materials might be tailored to specific needs at a fixed composition

*Corresponding author. Tel.: +34-91-394-4214; fax: +34-91-394-4352.
E-mail address: aguirrem@eucmos.sim.ucm.es (M.H. Aguirre).

0022-0248/03/$ - see front matter
doi:10.1016/S0022-0248(03)01236-3

without being necessary to introduce additional elements (dopants).

Although, molecular beam epitaxy (MBE) and organometallic vapour phase epitaxy (OMVPE) techniques are used to grow these metastable ordered alloys (because most thermodynamic parameters are controllable), we have grown our samples by the ISOVPE method [13] with which new CuPt and CuAu I-type structures have been found in HgCdTe.

The II–VI ternary compound $Hg_{1-x}Cd_xTe$ (MCT) is one of the most important semiconductors for infrared detection and thermal imaging [14,15]. In the present study, TEM investigations have been performed on the epitaxially grown MCT samples in order to acquire a better knowledge of its growth quality. The results using selected area electron diffraction pattern (SAED) and high-resolution TEM (HRTEM) image have shown for the first time a CuPt- and CuAu I-type ordering in $Hg_{1-x}Cd_xTe$ compounds.

2. Experimental procedure

The ISOVPE growth was performed in a two-zone furnace with a temperature gradient ranging from 400°C to 600°C. The growth temperature was 600°C. CdTe substrates in (1 1 0) and (1 1 1) orientations from eV PRODUCTS & Co. were used. HgCdTe epilayer thickness was between 50 and 100 μm. The composition was checked, in the first layer and in the cleaved film, by a Philips 505 scanning electron microscopy (SEM) with an EDAX 9100 electron microprobe.

Planar view and cross-section observation of the thin films were performed by TEM in a Jeol JEM 2000FX electron microscope and the composition was evaluated in situ by a Link Pentafet 5947 spectrometer (Oxford Microanalysis Group). A Jeol JEM 4000EX was used to obtain HRTEM images.

Thin crystals observed both in planar view and cross-sectional geometries were obtained by ion milling to electron transparency using Ar^+ ions. The samples were not cooled below room temperature during the milling. In the case of planar view, the thinning process starts from the CdTe substrate until the HgCdTe thin layer is reached, so that the top layer is preserved. In a cross-section analysis, the sample was thinned in a transverse section; so it is possible to study not only the surface epilayer, but also the substrate.

3. Results

A micrograph of the whole $Hg_{1-x}Cd_xTe$ sample can be seen in Fig. 1(a), where the surface epilayer presents constant composition $Hg_{0.8}Cd_{0.2}Te$ down

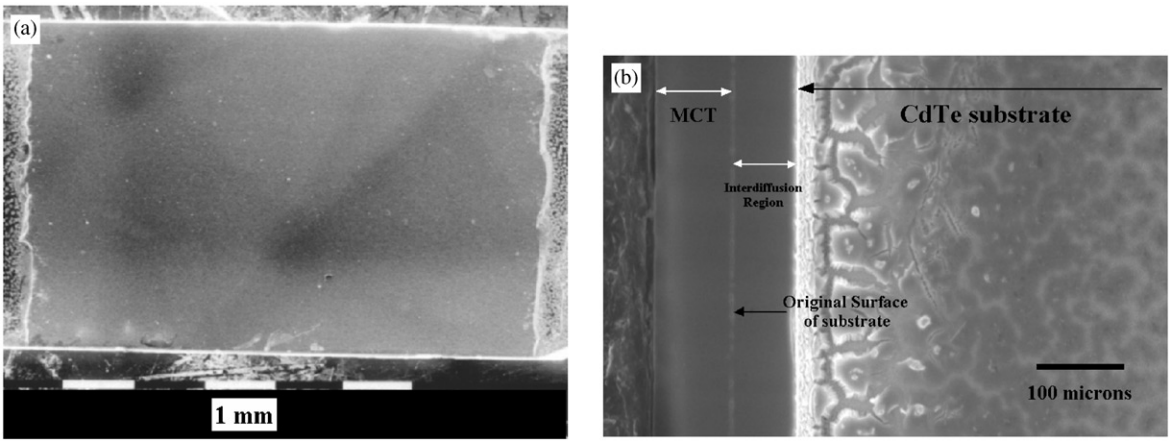

Fig. 1. (a) SEM micrograph of a whole sample in planar view and (b) cleaved sample showing the different parts of grown epilayer and CdTe substrate.

to 15–20 μm deep [16–18]. Then, the composition changes gradually from the surface epilayer ($x = 0.2$) to the CdTe/HgCdTe interface ($x = 1$). Fig. 1(b) shows a cleaved ([1 1 0] direction) epitaxially grown crystal, with a very different contrast between the MCT epitaxial film and the CdTe substrate. This variation is due to chemical etching using a Hähnert solution [19] for 10 s. The chemical etching solution also reveals the original surface of the CdTe substrate, being the boundary between the MCT region and the interdiffusion zone. A detailed study of a composition profile is given in Refs. [16–18].

Thin specimens with [1 1 1]- and [1 1 0]-growth axis were analysed in planar view geometry after a chemical polish with 2% bromine methanol solution. The diffraction pattern depicted in Fig. 2(a) was obtained with an incident electron beam parallel to the [1 1 0] direction. In the case of (1 1 0) epitaxial growth, the incident beam direction coincides with the growth axis, while for (1 1 1) epitaxial growth, an angle difference of 35.26° exists with respect to the [1 1 0] direction and this is reached by the double-tilting TEM holder. This specific diffraction pattern, shown in Fig. 2(a), was obtained for all the analysed growth samples (using both (1 1 1) and (1 1 0) CdTe substrates). This pattern is similar to the [1 1 0] zone axis in CuPt-type structure, where extra spots at $\frac{1}{2}\langle 1\,\bar{1}\,1\rangle$ and $\frac{1}{2}\langle \bar{1}\,1\,1\rangle$ appear. These spots reveal ordering in $\{1\,1\,1\}$ planes, where the repeated atomic sequence may be: CdTe/HgTe in [1 1 1] directions. Nevertheless, the mentioned ordering appears in two directions, suggesting the existence of two-microdomain variants, one in $\frac{1}{2}\langle 1\,\bar{1}\,1\rangle$ direction and the other in $\frac{1}{2}\langle \bar{1}\,1\,1\rangle$ direction [11]. In Fig. 2(b) a difference in contrast between both microdomains in a low-resolution image can be observed, where the microdomain size ranges between 10 and 20 nm. Fig. 2(c) shows one microdomain with high-resolution TEM, where the double periodicity of $\{1\,1\,1\}$ planes (7.4 Å) is clearly observed since the single distance between planes (1 1 1) is 3.7 Å. The cell parameter in $Hg_{1-x}Cd_xTe$ is $a \approx 6.46$ in zinc blend structure. The composition, where this superstructure region was found, ranged between $x = 0.35$ and $x = 0.65$.

The cross-section analysis of (1 1 0) samples was performed in three stages. The first analysis showed the CuPt-type ordered structure, diffraction pattern and low-resolution TEM image being similar to those of Fig. 2, but displaying in this case the [1 $\bar{1}$ 0] zone axis. The second analysis (SAED and HRTEM) was performed after a second ion-milling process of the same sample, which made possible the observation of inner layers. Unexpected results were obtained since not only CuPt-type ordered structures were found, but also CuAuI-type ordered structures appeared. In the third stage, to confirm the previous results, another (1 1 0) sample was thinned with this geometry, but analysing the [1 $\bar{1}$ 2] zone axis.

Fig. 3 shows the cross-section along the [1 $\bar{1}$ 0] zone axis after the second Ar^+ ion milling thinning, where (a) is the diffraction pattern and (b) the high-resolution image. Again, a CuPt-type ordered structure seems to appear by means of $\frac{1}{2}\{1\,1\,1\}$ pole diffraction. It can be observed that spots on the $\frac{1}{2}\langle \bar{1}\,\bar{1}\,1\rangle$ direction show a considerably higher intensity than those on the $\frac{1}{2}\langle 1\,1\,1\rangle$ direction. The large number of microdomains with the first direction superstructure can explain this fact.

The same SAED analysis also shows the spots on (0 0 1) and (1 1 0) that are extinctions of the zinc blend structure and confirm the presence of CuAu I-type ordered structure [9]. In this case, the atomic arrangements in $Hg_{1-x}Cd_xTe$ epitaxial layers are given by repetition of the CdTe/HgTe ordering along [0 0 1] and the [1 1 0] directions. HRTEM image (Fig. 3b) confirms that the ordered structures, CuAuI and CuPt types, and the zinc blend structure coexist with each other, forming microdomain sets.

In the third stage of analysis, the sample was analysed down the [1 $\bar{1}$ 2] zone axis. The diffraction pattern of this zone axis is shown in Fig. 4(a), presenting extra spots at $\frac{1}{2}(\bar{1}\,1\,1)$ and (1 1 0), indicating the existence of both CuPt- and CuAuI-type ordered structures, respectively. The corresponding HRTEM image (Fig. 4b) confirms the coexistence of these microdomain sets. The composition of this region was $Hg_{0.45}Cd_{0.55}Te$ ($\Delta x = 2\%$). Fig. 4b also shows an antiphase boundary and stress between zinc blend domains

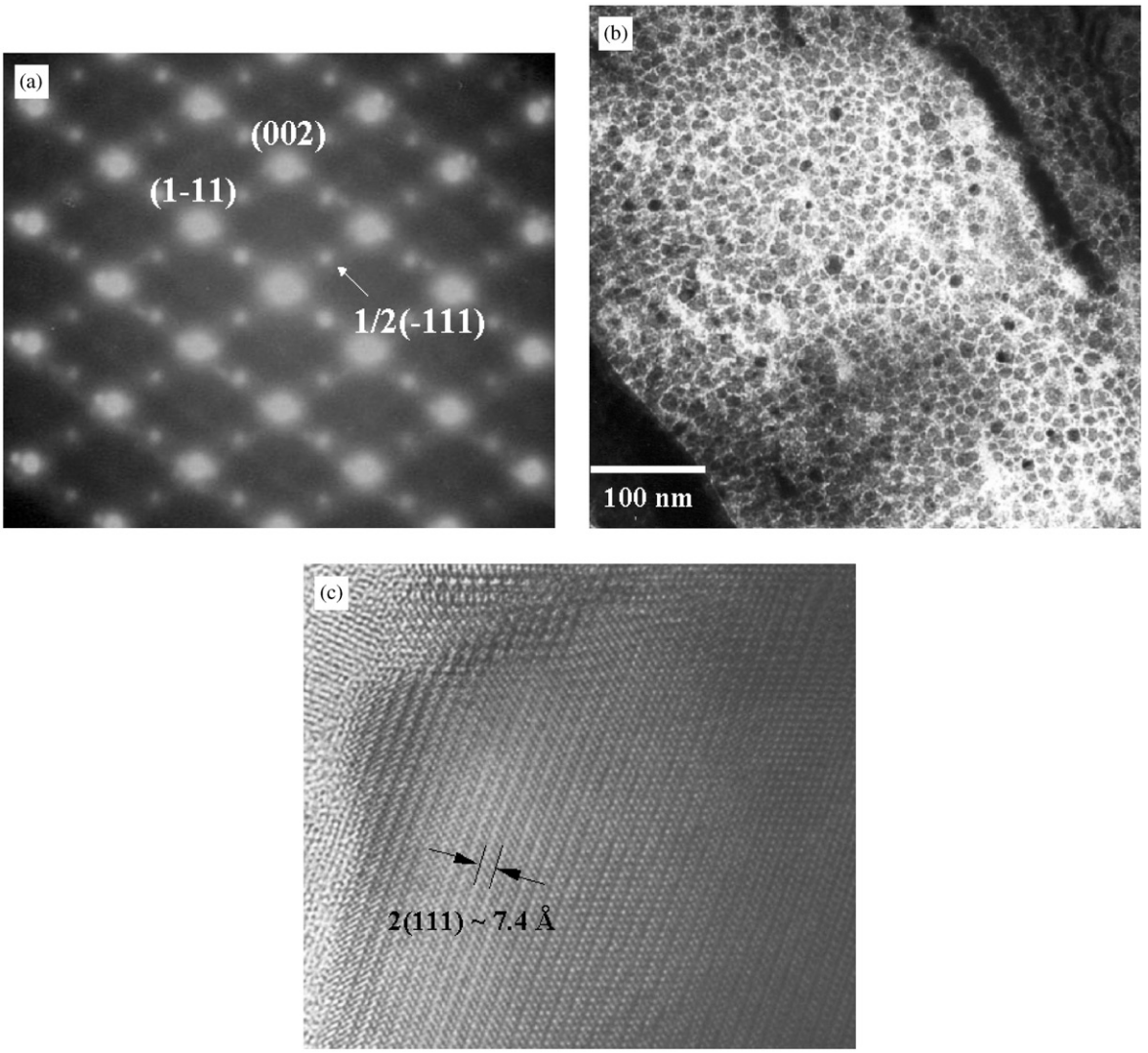

Fig. 2. (a) [1 1 0] Transmission electron diffraction (TED) pattern found in planar view geometry samples. $\frac{1}{2}(1\,\bar{1}\,1)$ and $\frac{1}{2}(\bar{1}\,1\,1)$ spots from CuPt-type superstructure are shown. (b) Low-resolution TEM image showing microdomains with different contrast. (c) High-resolution TEM image from one microdomain.

and zones with CuPt and CuAuI-type ordered structures.

4. Discussion

Although $Hg_{1-x}Cd_xTe$ epilayer with various Hg mole fractions were grown and analysed, only in regions with composition $x \approx 0.5$, the CuPt- and CuAuI-type ordered structures were found. This is because that specific composition is required to allow the atomic sequence CdTe/HgTe in the ordered structure. These ordered structures were not observed in $Hg_{1-x}Cd_xTe$ with a very low Cd mole fraction or a very low Hg mole fraction.

Ordering occurs in samples that are obtained under suitable growth parameters, i.e. by controlling mainly the growth temperature, the growth rate and substrate misorientation parameters. A study of the correlation between the growth

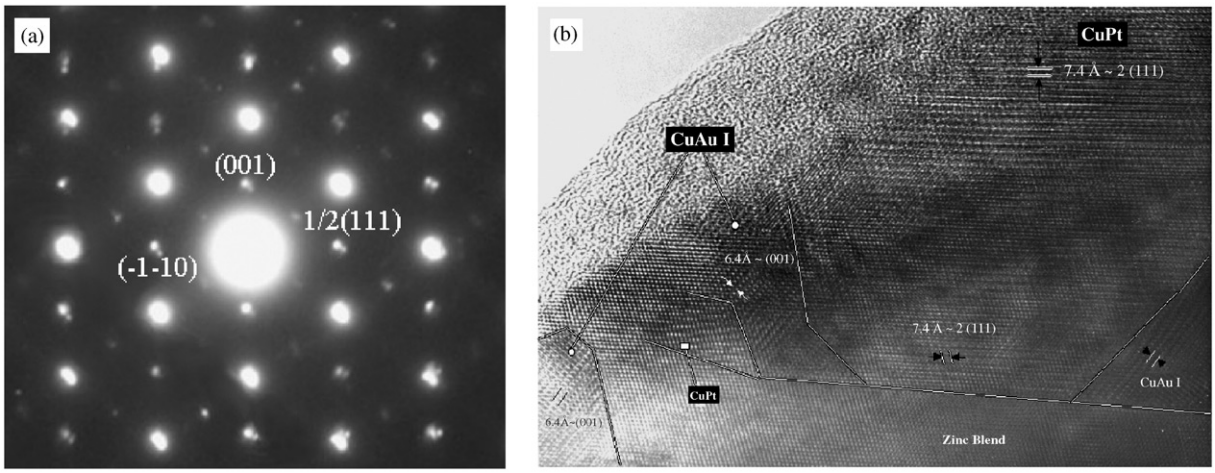

Fig. 3. (a) [1 $\bar{1}$ 0] SAED pattern from cross-sectional geometry, with coexisting CuPt- and CuAu I-type structures in microdomain sets. (b) High-resolution image corresponding to [1 $\bar{1}$ 0] SAED pattern.

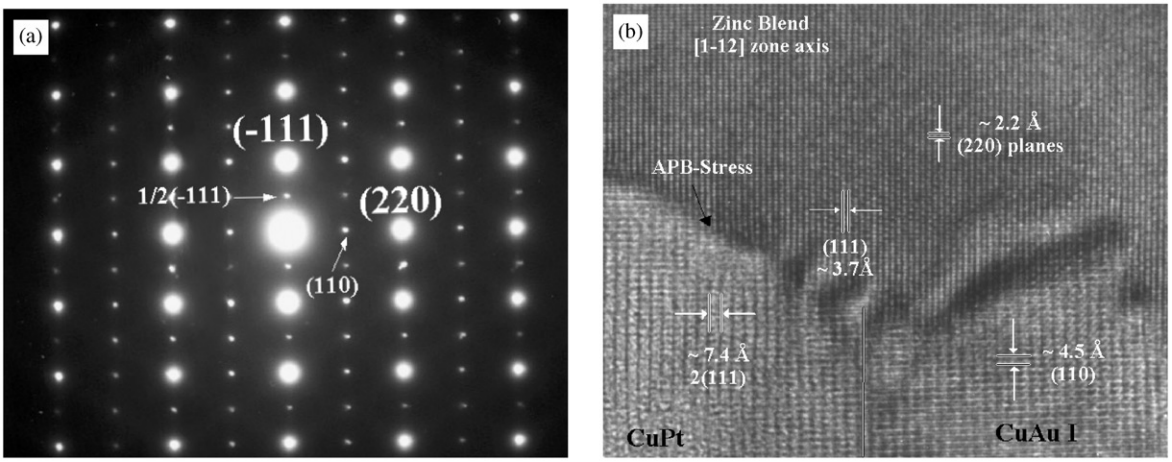

Fig. 4. (a) [1 $\bar{1}$ 2] SAED pattern corresponding to cross-sectional geometry with coexisting CuPt- and CuAu I-type structures in the microdomain set. (b) HRTEM image corresponding to [1 $\bar{1}$ 2] zone axis. An antiphase boundary exists between the zinc blend zone and CuPt–CuAuI zone with marked stress.

parameters and the degree of order would probably throw light on the ordering mechanism.

The exact mechanism for the spontaneous ordering formation during growth is not clearly known yet; however, acceptable models have been described elsewhere [20–23]. Experimental observations of the ordering phenomena seem to have different origins: e.g., it is observed that CuPt-type ordering in CdZnTe is concentrated near the interface region between CdZnTe and GaAs [11,12], where the factors producing the localised ordering are possibly related with the large lattice misfit or surface strain. The relaxation phenomenon near a heterointerface with large mismatch may influence the order–disorder transformation.

On the other hand, it is generally believed [21,24–26] that the origin of CuPt-type ordering in the epitaxial layer is associated with surface

reconstruction during growth. Le Goues et al. [27] proposed that the CuPt-type ordering observation in (0 0 1) MBE SiGe layer was a result of a subsurface lateral segregation of Si and Ge atoms. This seems to minimise the dimer-induced subsurface stress, which is present at (2×1) reconstructed growth surface. Norman et al. [1] extended this idea to III–V alloys.

The latter explanation of surface reconstruction seems to be more suitable for the material used in the present work and for the epitaxial growth method employed due to the small misfit (around 0.3% [16]) between CdTe and HgCdTe that would hardly generate strain.

The CuAu I superstructure has been found for III–V alloys grown onto (1 1 0) and (0 0 1) substrates [7]. The superstructures, CuPt in III–V and I–III–VI materials, have been obtained using (0 0 1) substrate [12] and [1 1 2] Si substrate [10], respectively. Therefore, the relationship between the surface reconstruction for different substrates and the obtained superstructure does not seem to be easy to predict. In this work, the CuPt superstructure was found in (1 1 1) and (1 1 0) grown samples, whilst CuAu I was only present on (1 1 0) HgCdTe-grown samples. More studies on surface reconstruction using different CdTe substrates, different surface preparations and types of growing methods are still necessary to give a reasonable explanation.

On the other hand, the possibility of some CuAu I ordering taking place during the thin foil preparation by means of ion milling has to be kept in mind. CuPt is unstable and the milling process introduces damage (as radiation damage), point defects and strain, increasing the rate of atomic rearrangement. As an example of another radiation damage process, it has been observed [10] that during irradiation with the electron beam, a transformation from a CuPt superstructure to a sphalerite or chalcopyrite phase has happened in $CuInSe_2$.

5. Conclusion

HgCdTe epitaxial growths, using both (1 1 1) and (1 1 0) substrates, have been studied by means of SAED and HRTEM techniques. To our knowledge, this is the first report on CuPt and CuAu I ordering in HgCdTe. CuPt ordering coexist with CuAu I ordering and with zinc blend structure.

The CuPt-type structure is confirmed as $\frac{1}{2}\{1\,1\,1\}$-pole diffraction in SAED pattern and HRTEM images corresponding to the [1 1 0], which show the double periodicity in the $\{1\,1\,1\}$ planes.

On the other hand, the $\{1\,1\,0\}$ and $\{1\,0\,0\}$ reflections present in $[1\,\bar{1}\,2]$ or the $\{1\,1\,0\}$ and $\{0\,0\,1\}$ in $[1\,\bar{1}\,0]$ SAED patterns confirm that CuAu I ordering was found in HgCdTe. It was carefully corroborated using HRTEM images that the extra reflections in the SAED patterns did not arise as double diffraction. Both structures were found only when the composition was near $x\approx0.5$, which means that the same mole fractions of Hg and Cd exist in the compound.

Acknowledgements

Dra. Myriam H. Aguirre thanks CONICET for the grant No. 403/97 that enabled her to accomplish this work. The authors are indebted to Prof. Miguel Ángel Alario-Franco for providing facilities at the Microscopy Centre "Luis Brú"-Universidad Complutense, Madrid (Spain).

References

[1] A. Norman, T. Seong, I. Fergusson, G. Booker, B. Joyce, Semicond. Sci. Technol. 8 (1993) S9.
[2] J. Martins, A. Zunger, Phys. Rev. Lett. 56 (1986) 1400.
[3] A. Mbaye, A. Zunger, D. Wood, Appl. Phys. Lett. 49 (1986) 782.
[4] D. Wood, A. Zunger, Phys. Rev. Lett. 61 (1998) 1501.
[5] S. Froyen, S. Wei, A. Zunger, Phys. Rev. B. Rapid Commun. 38 (1988) 10124.
[6] A. Zunger, D. Wood, J. Crystal Growth 98 (1989) 1.
[7] T. Kuan, T. Kuech, W. Wang, E. Wilkie, Phys. Rev. Lett. 54 (3) (1985) 201.
[8] H. Jen, M. Cherng, G. Stringfellow, Appl. Phys. Lett. 48 (23) (1986) 1603.
[9] A. Gomyo, T. Suzuki, S. Iijima, Phys. Rev. Lett. 60 (25) (1988) 2645.
[10] M. Bode, J. Appl. Phys. 76 (1) (1994) 159.

[11] M. Kwon, J. Lee, S. Suh, Jpn. J. Appl. Phys. 37 (1998) L21.
[12] H. Lee, J. Lee, T. Kim, D. Lee, D. Choo, H. Park, Appl. Phys. Lett. 79 (11) (2001) 1637.
[13] P. Becla, P.A. Wolff, R.L. Aggarawal, Y.S. Yuen, J. Vacuum Sci. Technol. A 3 (1985) 119.
[14] G. Destefanis, J. Crystal Growth 86 (1988) 700.
[15] L. Bubulac, J. Crystal Growth 86 (1988) 723.
[16] M. Aguirre, Ph.D. Thesis, Universidad de Buenos Aires, 2001.
[17] U. Gilabert, A. Trigubó, R. González, N.E. Walsöe de Reca, Defect Diffusion Forum 162–163 (1998) 1.
[18] U. Gilabert, A. Trigubó, R. González, N.E. Walsöe de Reca, Inorg. Mater. 34 (9) (1998) 890.
[19] I. Hähnert, M. Shenk, J. Crystal Growth 101 (1990) 251.
[20] J. Bernard, R. Dandrea, L. Ferreira, S. Fronyen, S. Wei, A. Zunger, Appl. Phys. Lett. 56 (8) (1990) 731.
[21] S. Froyen, A. Zunger, Phys. Rev. Lett. 66 (1991) 2132.
[22] S. Zhand, S. Froyen, A. Zunger, Appl. Phys. Lett. 67 (1995) 3141.
[23] S. Froyen, A. Zunger, Phys. Rev. B 53 (1996) 4570.
[24] I. Murgatroyd, A. Norman, G. Booker, J. Appl. Phys. 67 (1990) 2310.
[25] T. Suzuki, A. Gomyo, J. Crystal Growth 111 (1991) 353.
[26] G. Chen, D. Jaw, G. Stringfellow, J. Appl. Phys. 69 (1991) 4263.
[27] F. LeGoues, J. Kesan, S. Iyer, J. Tersoff, R. Tromp, Phys. Rev. Lett. 64 (1990) 2038.